Molecular Dynamics Simulation of Bisphenol A Polycarbonate

J. H. Shih and C. L. Chen*

Department of Chemistry, National Sun Yat-sen University, Kaohsiung, Taiwan 80424, ROC

Received November 8, 1994; Revised Manuscript Received April 17, 1995®

ABSTRACT: Molecular dynamics (MD) simulations of Bisphenol A polycarbonate are carried out with the TRIPOS 5.2 force field in a relatively short time of 80 ps at 300 and 400 K. Both structural and dynamical properties are analyzed. The configurations of the backbones, the phenylene rings, and the carbonate groups are investigated. The carbonate group is found to more easily undergo rotation than the isopropylidene group. The diffusion coefficients of the simulated motional units are approximately tripled when the temperature is increased from 300 to 400 K. The mobilities of the segments are dependent on the free volume of the motions. Cooperative motions between the phenylene rings as well as coupling motions between the phenylene ring and the carbonate group are examined. Long-range cooperativities of motions and interchain interactions are also investigated.

Introduction

Glassy Bisphenol A polycarbonate (BPAPC) has various applications due to its high glass transition temperature (414 K) and high melting point (498 K) in combination with its transparent property and good impact resistance. Structural properties and molecular motions of this polymer are very important in the investigation of the molecular origin of its mechanical properties. The structures of the analogues of BPAPC have been well characterized by X-ray diffraction,[1-5] neutron scattering,[6-9] and light scattering studies.[10-13] The small segmental motions and the molecular structures can be examined by various techniques such as NMR[14-31] and dielectric relaxation.[32-34] The NMR studies[14,15] show that the phenylene rings of BPAPC undergo primarily large-angle jumps between two sites whereas the backbone motions are quite restricted. Broad-band dielectric studies[32] show that the β-relaxation of BPAPC may be due to the coupling motions of the phenylene ring and the carbonate group. Infrared dichroism[35] and mechanical relaxation[36-38] have been applied to investigate the large segmental and main-chain motions. In the analyses of the dynamic mechanical spectra[37,38] of alternating copolymer and blend polymer, the results suggest that the second relaxation of BPAPC is due to the cooperative motion of several repeat units and the intermolecular interactions provide contributions to the molecular motions. The previous experimental results have been well reviewed by Hutnik et al.[39-42]

In addition to experimental efforts, theoretical calculations have been applied to assist in the identification of the possible structures and the feasible types of molecular motions in BPAPC. Methods of theoretical calculations include molecular mechanics[2,21,42-46] and quantum mechanical calculations.[47-52] In most calculations, analogues including diphenyl carbonate (DPC) and 2,2-diphenylpropane (DPP) are used to model BPAPC. Various semiempirical methods[47-51] and ab initio calculations[52] have been employed to study the rotational motions of the phenylene rings in BPAPC. Calculations are usually in agreement with the experimental results of small segmental motions. The drawback of the quantum mechanical studies is that the calculations are based on small isolated analogous compounds which do not account for the packing effects precisely and the segments may be too small to represent a polymer chain.

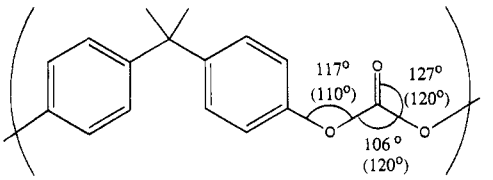

Figure 1. Repeating unit of BPAPC with the modified angles. The values of these angles of the original TRIPOS 5.2 force field are given in parentheses.

Recently, computer simulation[39,40,53-55] has been proved to be a very powerful tool in the investigations of the structures and dynamical properties of polymers. Brownian dynamics simulations on two-dimensional lattices of interacting benzene rings have been reported by Perchak et al.[53] Their results indicate that the flexibility of the lattice affects the ring-flipping motion. A quasi-static simulation of BPAPC has been reported by Hutnik et al.[40] This model is proved to be useful in modeling chain configurations. We have reported a full-scale MD simulation of amorphous poly(phenylene oxide) (PPO).[54] The simulation indicates that the cooperativities commonly exist between phenylene rotations and between backbone wiggles. Herein, we report the MD simulations of amorphous BPAPC, in which the segmental structures and dynamics of BPAPC are analyzed. The results are compared with the experimental observations and the earlier related calculations.

System and Method

1. Force Field. The modified TRIPOS 5.2 force field is used to carry out the MD simulations. In the modified force field the force field parameters are the same as the ones of the original TRIPOS force field[56] except that the bond angles in the carbonate group are different. The equilibrium bond angles in the carbonate group of BPAPC are adopted from the results of X-ray diffraction of DPBC.[1] The potential comprises van der Waals, bond stretch, angle bending, torsional, and out-of-plane bending terms. The reason for choosing this force field is based on its simplicity and accuracy. Given in Figure 1 is the repeating unit of BPAPC with these modified angles. The original values of the TRIPOS 5.2 force field are also given in the parentheses.

* To whom correspondence should be sent.
® Abstract published in *Advance ACS Abstracts,* June 1, 1995.

0024-9297/95/2228-4509$09.00/0

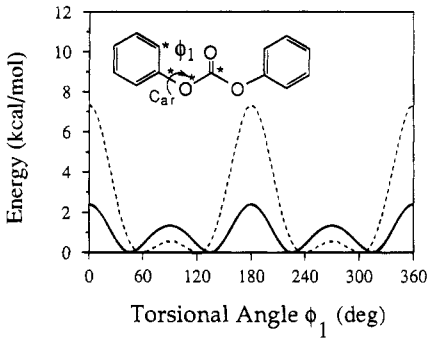

Figure 2. Minimum energy curves for a phenyl ring rotation around the C_{ar}–O bond in DPC. The torsional angle ϕ_1 is defined by the sequentially marked atoms. The solid and dashed lines represent the energy curves calculated by the modified and original TRIPOS force fields, respectively.

Figure 2 shows the calculated minimum energy curves for a phenyl ring rotation around the C_{ar}–O bond in model compound DPC with use of the original TRIPOS force field and the modified force field. In the figure, the torsional angle ϕ_1 is defined by the sequentially marked atoms. The minimum energy of a specified torsional angle, ϕ_1, is obtained by relaxing the other degrees of freedom to their optimum values. The figure shows that the original TRIPOS force field (dashed line) and the modified force field (solid line) give the energy barrier of 7.2 and 2.3 kcal/mol, respectively. Hutnik et al. had calculated this energy barrier, and their results give a barrier of 3.3 kcal/mol.[42] Sun et al. reported that the calculated energy barrier is 1.5 kcal/mol for the same motion.[43] Therefore the modified force field gives better agreement in comparison with the calculated results of Hutnik's and Sun's force fields. Hutnik et al. and Sun et al. also estimated the energy difference between the trans–trans and trans–cis conformations of DPC. Their values of energy differences are 1.7 and 2.6 kcal/mol,[42,43] respectively. The modified force field gives an energy difference of 2.1 kcal/mol. Therefore, this modified force field is appropriate to use in the simulation.

2. Initial BPAPC Chain. Our BPAPC chain is composed of 31 repeating units with diphenylisopropylidene units attached to both ends. The chain contains 64 phenylene rings and 32 carbonate linkage units in total. To avoid overcrowded BPAPC at the beginning of the MD simulation, a special BPAPC system setup process is required. The initial BPAPC chain is straight-extended with all trans–trans conformations, equilibrium bond angles, and equilibrium bond distances. This BPAPC chain is put into a cubic box with the box dimension larger than the size of the chain. The initial velocities of all atoms are randomly generated from a Gaussian distribution.

3. Preparation of the Solid Amorphous System. The solid amorphous system is prepared by the gradual volume reduction method as described in our previous PPO study.[54] First, the MD simulation is carried out on the initial BPAPC system until the system is in equilibrium. The equilibrium means that the kinetic energy of the system fluctuates within 10% of a predetermined range around $3Nk_bT/2$, where N is the total number of atoms in the system, k_b is the Boltzmann constant, and T is the absolute temperature. After the equilibrium, the MD simulation is carried out for another 5 ps to make sure that the system is truly in the equilibrium condition. The size of the box is then reduced to 95% of its original size in three dimensions.

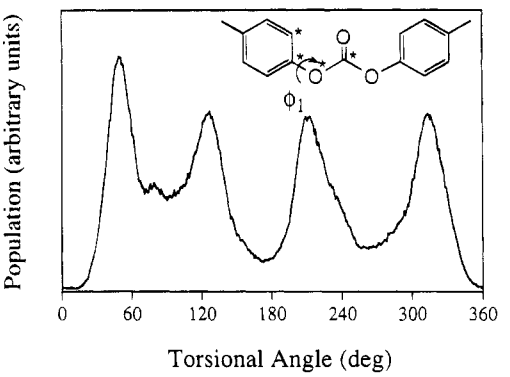

Figure 3. Population of the torsional angle ϕ_1 at 400 K. ϕ_1 is defined by the marked atoms.

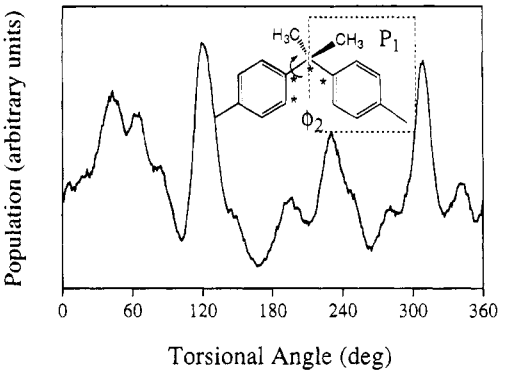

Figure 4. Population of the torsional angle ϕ_2 at 400 K. ϕ_2 is defined by the marked atoms. P_1 denates the plane which bisects the CH_3–C–CH_3 angle.

The MD simulation is carried out until the system reaches a new equilibrium condition. The box-reducing process is repeated until the density of the system reaches the reported glassy-state density, 1.20 g/cm^3.

4. Simulation Conditions. The MD simulations are carried out on a CONVEX C3840 computer. Two temperatures, 300 and 400 K, are chosen in the simulation. Both temperatures are lower than the glass transition temperature (T_g) of BPAPC. The Beeman algorithm[57] is used to integrate the equation of motion. A cutoff distance of 10.2 Å and a three-dimensional periodic boundary condition are selected. A relatively small time step, 0.2 fs, is used in the integrations because of the fast vibration of the CH bond. After the system reaches equilibrium, trajectories of 80 ps duration are recorded and analyzed. In the simulations, we found that the total energy of the system fluctuates less than 0.1% of the total energy.

Results and Discussion

1. Structures. In this simulation, the structural properties at 300 and 400 K are found to be very similar; hence, we only report the results at 400 K. Figures 3–7 show the relative populations of the values of five types of torsional angles at 400 K. The population of the value of a specified angle is obtained from counting the occurrences of the value of the angle in 80 ps. In these figures, each torsional angle, ϕ, is defined by the sequentially marked atoms. For convenience, phenylene rings are numbered from 1 to 64 along the chain.

Figure 3 shows the populations of ϕ_1. The torsional angle ϕ_1 is defined by the relative orientation of the planes of the phenylene ring and the carbonate group. The significant populations of ϕ_1 are around 49, 127, 211, and 313°. These populations correspond to the

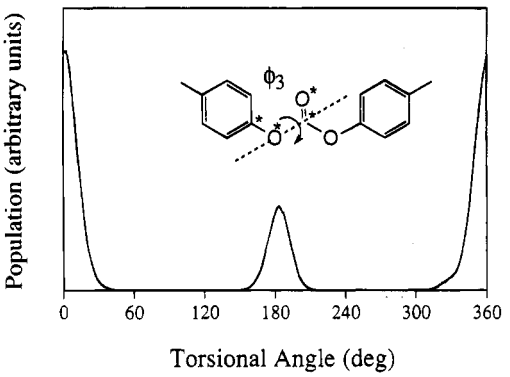

Figure 5. Population of the torsional angle ϕ_3 at 400 K. ϕ_3 is defined by the marked atoms.

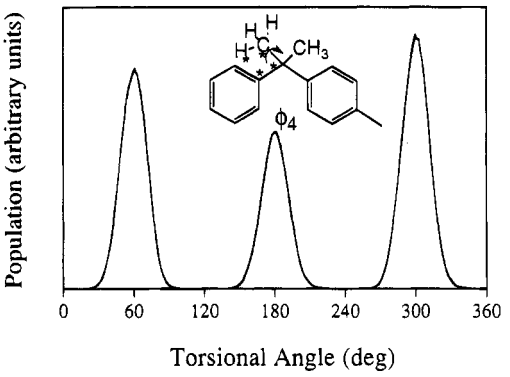

Figure 6. Population of the torsional angle ϕ_4 at 400 K. ϕ_4 is defined by the marked atoms.

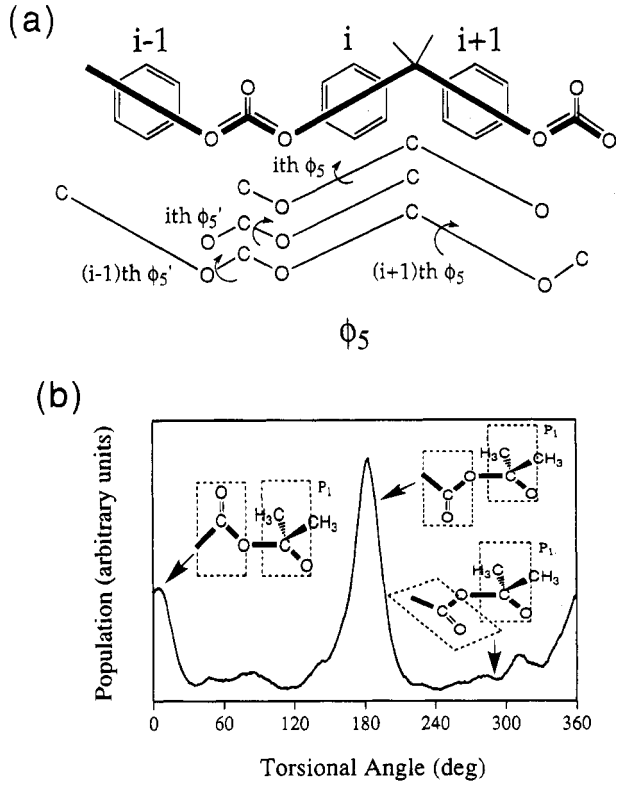

Figure 7. (a) Illustration of the torsional angle ϕ_5. ϕ_5 is defined by the four sequential atoms located on the backbone. (b) Population of the torsional angle ϕ_5 at 400 K.

phenylene ring tilting to the carbonate group with an angle of 49, 53, 31, and 47°. The largest population of ϕ_1 is around 49°. In addition to the angles mentioned above, we also found that ϕ_1 has some significant population around 90°. The light scattering[10] and the neutron diffraction[7] of the DPC crystal reveal that ϕ_1 is 46 and 45°. The X-ray diffraction[1] of DPBC shows that the values of ϕ_1 are 48° and around 90°. The ϕ_1 calculated by various methods for the most stable configurations ranged from 44 to 65°.[42,43,46-49] Therefore, our result of ϕ_1 agrees well with both experimental observations and calculations. The smallest population of ϕ_1 is around 0° (or 180°), which corresponds to a coplanar structure of the phenylene ring and the carbonate group. This is due to the strong repulsive interaction between the ortho hydrogen atom on the phenylene ring and the oxygen atom on the carbonate, which inhibits the coplanar structure.[1]

Given in Figure 4 are the populations of ϕ_2. The ϕ_2 is the torsional angle defined by the relative reorientation of the phenylene ring and the plane P_1 which bisects the CH_3-C-CH_3 angle of the isopropylidene unit. The significant populations of ϕ_2 are found around 43, 66, 119, 231, and 307°. These angles correspond to the phenylene ring tilting to the plane P_1 with an angle of 43, 66, 61, 51, and 53°. The X-ray determination of crystalline DPBC shows that the tilted angles are 61 and 36°.[1] The light scattering[10] and neutron scattering[7] experiments of the DPP crystal show that the tilted angles are around 48 and 45°. The calculated values of ϕ_2 for the most stable configurations of DPP ranged from 45 to 60°.[10,42,43,47,49] Therefore, our simulated angle of ϕ_2 also agrees well with both experimental observations and theoretical calculations. The results of populations of ϕ_1 and ϕ_2 indicate that the phenylene rings tilt to the carbonate group and to the plane P_1, respectively. The agreement between this simulation and model compound calculations in the configuration of the phenylene ring implies that the configuration of the phenylene ring is determined by the interactions of the ring and its neighboring groups. The packing effect is not important for this local structure.

Given in Figure 5 is the population of ϕ_3. The torsional angle ϕ_3 is defined by four sequential atoms which are the (O=)CO atoms on the carbonate group and the C atom on the phenylene ring attached to the carbonate group. Two dominant populations of this angle are found around 0 (360) and 180°. The 0 (360) and 180° of ϕ_3 correspond to the trans and cis conformations of the backbone, respectively. The figure shows that the population of the trans conformation is larger than the cis conformation. The figure also indicates that there are no trans–cis or cis–trans conversions in the glassy state because no population is detected between the cis and trans states. Various experiments[7,10,20,21] and simulations[42] also showed that the trans conformation of the carbonate group is more preferable than the cis conformation. Therefore, our result agrees with these experimental and simulated results.

Given in Figure 6 is the population of ϕ_4. ϕ_4 is the torsional angle defined by four sequential atoms, the selected atoms, the selected H atom and the C atom on the methyl group, the central isopropyl C atom, and the C atom on the phenylene ring which is attached to the isopropylidene group. The figure shows that ϕ_4 has large populations around 60, 180 and 300°. These angles of ϕ_4 correspond in the gauche and the trans conformations. The 3-fold rotation of the methyl group[16,22,23] has been proposed by various experiments and the rotational energy barrier is deduced as 4–6 kcal/mol.[22,23] This high rotational barrier is reported to be due to the presence of two methyl groups bound

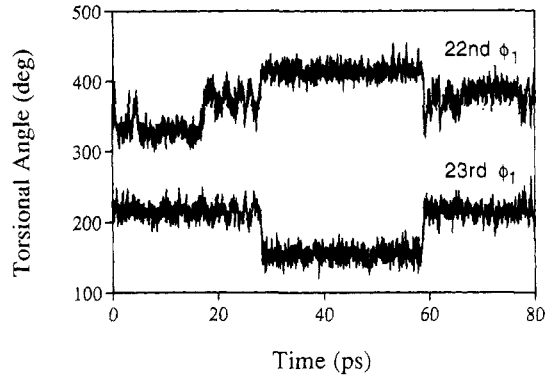

Figure 8. Trajectories of ϕ_1 of the 22nd and the 23rd phenylene rings at 400 K.

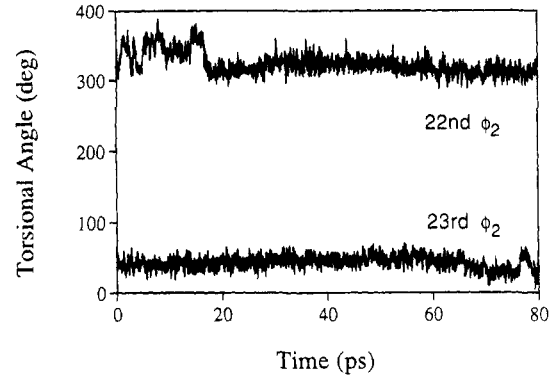

Figure 9. Trajectories of ϕ_2 of the 22nd and the 23rd phenylene rings at 400 K.

to the same carbon atom.[16] The coupling between the methyl group and the phenylene ring may also inhibit the internal rotation of the methyl group. In our simulation, we do not find this 3-fold rotation of the methyl group. This may be due to the overestimated parameters used in the simulation for the methyl group, or it may be that our simulated time is not long enough to observe this motion. Nevertheless, the rotation of the methyl group is demonstrated to have little effect on the surrounding matrix.[22] Therefore, we do not attempt to adjust our parameters or extend our simulation to check this methyl rotation.

Given in Figure 7a is the illustration of the angle of ϕ_5. ϕ_5 is the torsional angle defined by the four sequential atoms located on the backbone. Given in Figure 7b is the population of ϕ_5. The figure shows that the largest population of ϕ_5 is around 180°. The other significant population of ϕ_5 is around 0° (or 360°). These angles of ϕ_5 correspond to the trans (180°) and cis (0 and 360°) conformations of the backbone. These configurations all correspond to a coplanar arrangement of the carbonate group and the P_1 plane. The figure indicates that the trans conformation of the backbone is more favored than the cis.[5,6,44] The analysis of ϕ_3, which also represents part of the backbone configuration, shows that ϕ_3 populates only around either 180 or 0°. However, in Figure 7b, besides the trans and the cis conformations, some additional populations of ϕ_5 are found. These populations result from the tilted configuration between the carbonate group and the P_1 plane.

2. Short-Range Dynamics. Given in Figure 8 are the trajectories of the ϕ_1's of the 22nd and the 23rd phenylene rings. The figure shows that these two angles change simultaneously around 28 and 59 ps. At first glance, this looks like a cooperative rotation of the two phenylene rings. Given in Figure 9 are the trajectories of the ϕ_2's of the 22nd and 23rd phenylene rings. The figure shows that there are no significant angle changes around 28 and 59 ps. Therefore, the simultaneous angle changes in Figure 8 are due to the wagging motion of the carbonate group. Given in Figure 10 are the trajectories of ϕ_5 associated with the 22nd and the 23rd phenylene rings. The figure shows that the ϕ_5's change significantly around 28 and 59 ps. This is additional evidence to support that the simultaneous change of ϕ_1 is actually the wagging motion of the carbonate group. In Figure 8, there are no significant angle changes before 28 ps for the 23rd phenylene ring. Figures 8 and 9 show that both ϕ_1 and ϕ_2 of the 22nd phenylene ring undergo significant changes around 18 ps. These changes indicate independent rotation of the 22nd phenylene ring. The magnitude of the rotation of

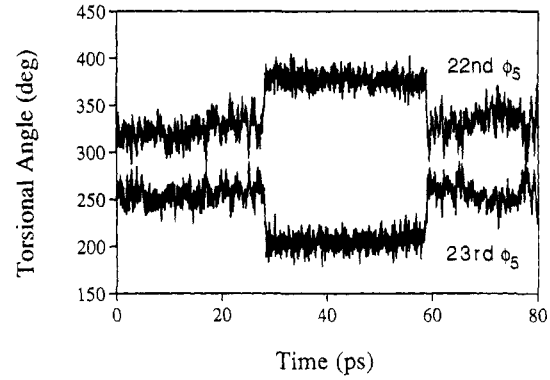

Figure 10. Trajectories of ϕ_5 of the 22nd and the 23rd phenylene rings at 400 K.

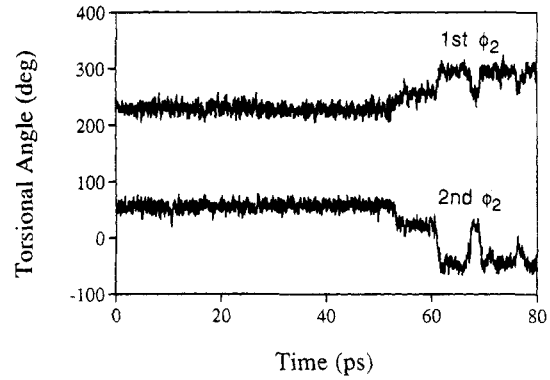

Figure 11. Trajectories of ϕ_2 of the 1st and the 2nd phenylene rings at 400 K.

the 22nd phenylene ring is found from Figure 8 to be about 80°. We also found, after this independent ring rotation, the neighboring carbonate group rotates. A similar type of coupled rotations of the phenylene ring and its neighboring carbonate group has been proposed in a quasi-static simulation.[40] Tekely and Turska also suggest that this type of coupled motion may be the origin of the narrowing line width of the NMR in the vicinity of −60 °C.[21]

Given in Figure 11 are the trajectories of the ϕ_2's of the 1st and 2nd phenylene rings attached to the 1st isopropylidene unit. The figure shows that ϕ_2 of ring 1 changes from 60 to −50° between 55 and 80 ps, while the ϕ_2 of the second ring changed in the same direction within the same duration. This is an in-phase[54] cooperative rotation of the rings attached to the same isopropylidene unit. This type of cooperative motion is also found between the 57th and 58th phenylene rings (not shown). The ϕ_2 of the 57th ring changes from 120

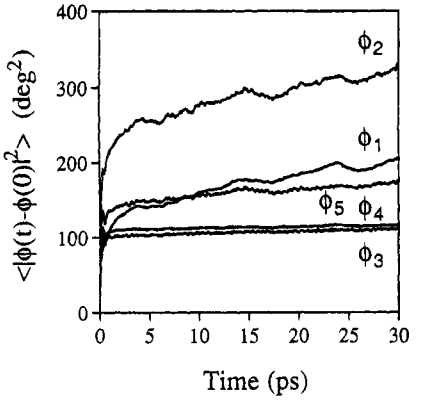

Figure 12. Mean square displacements of various torsional angles at 300 K.

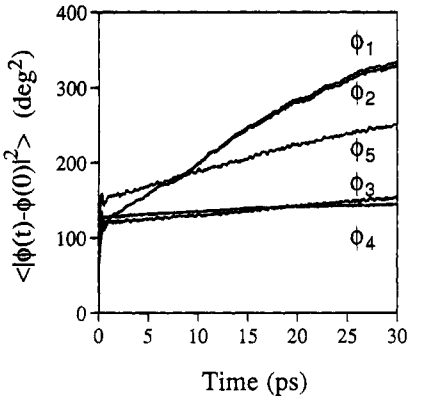

Figure 13. Mean square displacements of various torsional angles at 400 K.

to 40° at 65 ps, while the ϕ_2 of the 58th ring changes simultaneously from 160 to 20°. The reason for cooperative rotation may be due to the strong repulsive interaction between the ortho hydrogen atoms on the separated phenylene rings. The early molecular mechanics[21,46] and quantum mechanical[47] calculations of polycarbonate analogues show that this cooperative motion is favored energetically. In a recent MD simulation of amorphous PPO,[54] we have found that this in-phase cooperative rotation of two phenylene rings attached to the same linked atom occurs commonly.

On inspection of all the trajectories of the ϕ_5's, some significant and simultaneous changes of two different ϕ_5's are found. Those changes happened when the two angles share the same carbonate group. Figure 10 illustrates this phenomenon. This figure indicated that the angle changes of the 22nd and 23rd ϕ_5's at 28 and 59 ps are due to the reorientation of the shared carbonate group, which tells us that the carbonate group can more easily undergo rotation than the isopropylidene group. This may be realized from the viewpoint of free volume. The rotation of the isopropylidene unit will involve a large volume change. This is hindered by its environment. On the other hand, the carbonate unit is smaller and should more easily rotate in the amorphous solid.

To compare the mobility of the various motional units in BPAPC, the rotational diffusion coefficient, D, for each different type of rotation is evaluated by the equation

$$2Dt = \lim_{t\to\infty}\langle|\phi(t) - \phi(0)|^2\rangle$$

where ϕ is the corresponding rotational angle and the term in brackets denotes the mean square displacement of the angle. The magnitude of the diffusion coefficient reflects the mobility of the motional unit. Given in Figures 12 and 13 are the plots of the mean square displacements vs time for the analyzed torsional angles at 300 and 400 K, respectively. The diffusion coefficient is obtained from the slope of the mean square displacement with respect to the time. The slope is obtained from a linear least-squares fitting of the curves within the time range 5–30 ps. Table 1 lists the values of these diffusion coefficients for all of the torsional angles. The table shows that all of these diffusion coefficients approximately tripled when the temperature was increased from 300 to 400 K. ϕ_1 and ϕ_2 are referred to the motion of a single ring, ϕ_3 is referred to the motion of a large segment, ϕ_4 is referred to the rotation of the methyl group, and ϕ_5 is referred to the motion of the backbone. Since ϕ_4 is referred to the rotation of the methyl group on the isopropylidene group, this rotation is inhibited by the other methyl group and the phenylene rings attached to the same isopropylidene group. Therefore, the diffusion coefficient of ϕ_4 shows the smallest value among all ϕ's. As usual, D's are related to the free volume for the motion. Figure 14 illustrates the free volume for the different types of motions. ϕ_1 and ϕ_2 have larger D values due to the smaller free volume, and ϕ_3 and ϕ_5 have smaller D values due to the larger free volume.

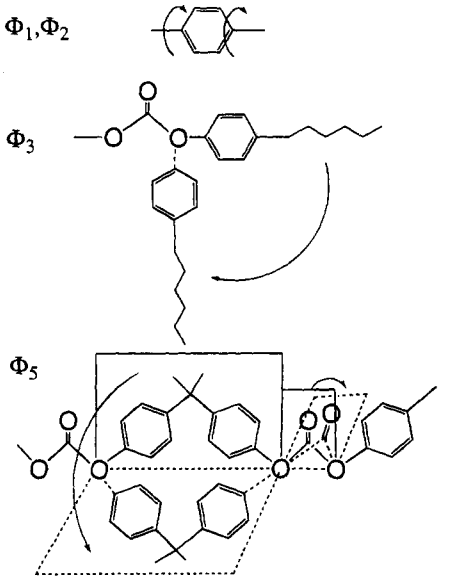

Figure 14. Illustration of the free volume of the motion of different segments.

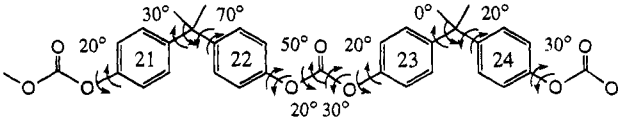

Figure 15. Approximate angle changes of the 21st–24th phenylene rings within 17–18 ps at 400 K.

Table 1. Rotational Diffusion Coefficients (deg²/ps) of Five Types of Motion

T(K)	ϕ_1	ϕ_2	ϕ_3	ϕ_4	ϕ_5
300	1.37	1.25	0.15	0.10	0.48
400	3.80	3.70	0.59	0.28	1.72

3. Long-Range Interactions. Given in Figure 15 are the angle changes of the segment composed of the 21st to 24th phenylene rings within 17–18 ps. The double arrows in the figure indicate the directions of

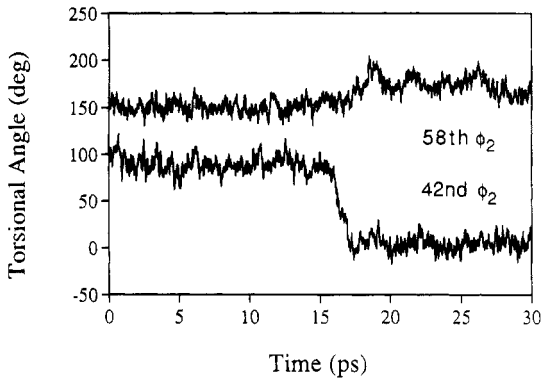

Figure 16. Trajectories of ϕ_1 of the 42nd and the 58th phenylene rings at 400 K.

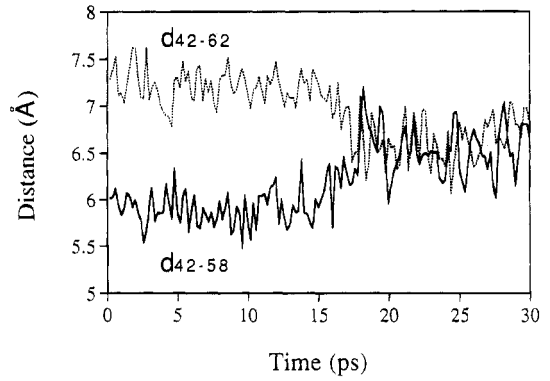

Figure 17. Center–center distances of the 42nd–58th and 42nd–62nd phenylene rings.

the rotations. The figure shows that the cooperative motion may extend to two repeating units (4 phenylene rings). In this motion, the phenylene rings on both sides of the carbonate unit rotate when the carbonate rotates. This result agrees with the result of the quasi-static simulation.[40] We do not find any other significant cooperative motion of a segment more than two repeating units from our simulations.

Given in Figure 16 are the trajectories of the ϕ_2's of the 42nd and the 58th phenylene rings. Given in Figure 17 are the distances, d_{42-58} and d_{42-62}, between the 42nd phenylene ring and the 58th and 62nd phenylene rings. The distance is evaluated from the distance between the centers of the rings. d_{42-58} is about 6 Å and d_{42-62} is about 7 Å before 17 ps. Both the 58th and 62nd phenylene rings are pretty close to the 42nd phenylene ring. Figure 16 shows that the 42nd phenylene ring undergoes 100° rotation around 17 ps. The 58th phenylene ring rotates after this time. This can be considered as an interchain cooperative motion. Figure 17 shows that, after the rotation of the 42nd phenylene ring, the 58th phenylene ring moves away and the 62nd phenylene ring moves closer. It shows that the 42nd ring repels the neighboring rings to generate free volume for rotation. After the rotation, other rings move closer to take the vacancy produced by the rotation. This analysis shows that the rotation of a ring would affect other rings within 7 Å.

4. Comments on the Conformational Transitions. In reality, the characteristic time of ring flip and conformational transitions of other segments in BPAPC is in the scale of microseconds. In our simulation of 80 ps, we found most of the phenylene rings and other segments oscillated with small amplitude around their equilibrium positions. In addition to this, a few conformational transitions of phenylene rings and other segments are accidentally detected. We realize that in this short-time simulation the probability of conformational changes should be very small in our simulated system. These detected conformational transitions may be due to the use of unimperfect force field. However, this report shows what kind of conformational transition may occur in BPAPC and what is the consequence after the conformational transition.

Conclusions

Amorphous BPAPC is simulated by using the MD method. Based on the trajectory analysis, our simulated molecular structures of amorphous BPAPC are in good agreement with both the experimental results and previous related calculations. The carbonate group is found easy to rotate. This should not be confused with the cooperative rotations of the attached phenylene rings. We found that the cooperative rotations are usually observed for the isopropylidene-linked phenylene rings. The coupling motion between the phenylene ring and its attached carbonate group is observed. The diffusion coefficients for the simulated motional units are approximately tripled when the temperature is increased from 300 to 400 K. The mobilities of the various motional units are estimated from the simulated diffusion coefficients. The mobility is related to the free volume of the motion. Long-range cooperative motions are observed for a segment composed of two repeating units. The rotation of the phenylene ring affects its neighboring rings.

Acknowledgment. Thanks are due to the Computer Center of NSYSU for their help during this work. This work is financially supported by Contract No. NSC-83-0208-M-110-023 from the National Science Council, ROC. We wish to thank Dr. C. C. Tung (NSYSU) for help in reviewing this paper. Valuable comments from one of the reviewers are greatly appreciated.

References and Notes

(1) Perez, S.; Scaringe, R. P. *Macromolecules* **1987**, *20*, 68.
(2) Henrichs, P. M.; Luss, H. R.; Scaringe, R. P. *Macromolecules* **1989**, *22*, 2731.
(3) Mitchell, G. R.; Windle, A. H. *Colloid Polym. Sci.* **1985**, *263*, 280.
(4) Schubach, H. R.; Heise, B. *Colloid Polym. Sci.* **1986**, *264*, 335.
(5) Turska, E.; Hurek, J.; Zmudzinski, L. *Polymer* **1979**, *20*, 321.
(6) Červinka, L.; Fischer, E. W.; Hahn, K.; Jiang, B.-Z.; Hellmann, G. P.; Kuhn, K.-J. *Polymer* **1987**, *28*, 1287.
(7) Červinka, L.; Fischer, E. W.; Dettenmaier, M. *Polymer* **1991**, *32*, 12.
(8) Ballard, D. G. H.; Burgess, A. N.; Cheshire, P.; Janke, E. W.; Nevin, A.; Schelten, J. *Polymer* **1981**, *22*, 1353.
(9) Floudas, G.; Higgins, J. S.; Meier, G.; Kremer, F.; Fischer, E. W. *Macromolecules* **1993**, *26*, 1676.
(10) Erman, B.; Marvin, D. C.; Irvine, P. A.; Flory, P. J. *Macromolecules* **1982**, *15*, 664.
(11) Erman, B.; Wu, D.; Irvine, P. A.; Marvin, D. C.; Flory, P. J. *Macromolecules* **1982**, *15*, 670.
(12) Floudas, G.; Lappas, A.; Fytas, G.; Meier, G. *Macromolecules* **1990**, *23*, 1747.
(13) Dettenmaier, M.; Kausch, H. H. *Colloid Polym. Sci.* **1981**, *259*, 209.
(14) Roy, A. K.; Jones, A. A.; Inglefield, P. T. *Macromolecules* **1986**, *19*, 1356.
(15) Schaefer, J.; Stejskal, E. O.; Mckay, R. A.; Dixon, W. T. *Macromolecules* **1984**, *17*, 1479.
(16) Tekely, P. *Macromolecules* **1986**, *19*, 2544.
(17) Schmidt, A.; Kowalewski, T.; Schaefer, J. *Macromolecules* **1993**, *26*, 1729.
(18) Spiess, H. W. *Colloid Polym. Sci.* **1983**, *261*, 193.
(19) Henrichs, P. M.; Linder, M.; Hewitt, J. M.; Massa, D.; Isaacson, H. V. *Macromolecules* **1984**, *17*, 2412.

(20) Henrichs, P. M.; Luss, H. R. *Macromolecules* **1988**, *21*, 860.
(21) Tekely, P.; Turska, E. *Polymer* **1983**, *24*, 667.
(22) Henrichs, P. M.; Nicely, V. A. *Macromolecules* **1991**, *24*, 2506.
(23) Ngai, K. L.; Rendell, R. W.; Yee, A. F. *Macromolecules* **1988**, *21*, 3396.
(24) Walton, J. H.; Lizak, M. J.; Conradi, M. S.; Cullion, T.; Schaefer, J. *Macromolecules* **1990**, *23*, 416.
(25) Henrichs, P. M.; Nicely, V. A. *Macromolecules* **1990**, *23*, 3193.
(26) Inglefield, P. T.; Jones, A. A.; Lubianez, R. P.; O'Gara, J. F. *Macromolecules* **1981**, *14*, 288.
(27) Jones, A. A.; O'Gara, J. F.; Inglefield, P. T.; Bendler, J. T.; Yee, A. F.; Ngai, K. L. *Macromolecules* **1983**, *16*, 568.
(28) Schaefer, J.; Stejskal, E. O.; Perchak, D.; Skolnick, J.; Yaris, R. *Macromolecules* **1985**, *18*, 368.
(29) Hansen, M. T.; Boeffel, C.; Spiess, H. W. *Colloid Polym. Sci.* **1993**, *271*, 446.
(30) Hansen, M. T.; Blümich, B.; Boeffel, C.; Spiess, H. W. *Macromolecules* **1992**, *25*, 5542.
(31) Hansen, M. T.; Kulik, A. S.; Prins, K. O.; Spiess, H. W. *Polymer* **1992**, *33*, 2231.
(32) Katana, G.; Kremer, F.; Fischer, E. W.; Plaetschke, R. *Macromolecules* **1993**, *26*, 3075.
(33) Watts, D. C.; Perry, E. P. *Polymer* **1978**, *19*, 248.
(34) Tiller, A. R. *Macromolecules* **1992**, *25*, 4605.
(35) Lunn, A. C.; Yannas, I. V. *J. Polym. Sci., Polym. Phys. Ed.* **1972**, *10*, 2189.
(36) Yee, A. F.; Smith, S. A. *Macromolecules* **1981**, *14*, 54.
(37) Jho, J. Y.; Yee, A. F. *Macromolecules* **1991**, *24*, 1905.
(38) Xiao, C.; Yee, A. F. *Macromolecules* **1992**, *25*, 6800.
(39) Hutnik, M.; Argon, A. S.; Suter, U. W. *Macromolecules* **1993**, *26*, 1097.
(40) Hutnik, M.; Argon, A. S.; Suter, U. M. *Macromolecules* **1991**, *24*, 5970.
(41) Hutnik, M.; Gentile, F. T.; Ludovice, P. J.; Suter, U. W.; Argon, A. S. *Macromolecules* **1991**, *24*, 5962.
(42) Hutnik, M.; Argon, A. S.; Suter, U. W. *Macromolecules* **1991**, *24*, 5956.
(43) Sun, H.; Mumby, S. J.; Maple, J. R.; Hagler, A. T. *J. Am. Chem. Soc.* **1994**, *116*, 2978.
(44) Williams, A. D.; Flory, P. J. *J. Polym. Sci., Polym. Phys. Ed.* **1968**, *6*, 1945.
(45) Tonelli, A. E. *Macromolecules* **1972**, *5*, 558.
(46) Sundararajan, P. R. *Can. J. Chem.* **1985**, *63*, 103.
(47) Sung, Y. J.; Chen, C. L.; Su, A. C. *Macromolecules* **1990**, *23*, 1941.
(48) Bicerano, J.; Clark, H. A. *Macromolecules* **1988**, *21*, 585.
(49) Laskowski, B. C.; Yoon, D. Y.; McLean, D.; Jaffe, R. L. *Macromolecules* **1988**, *21*, 1629.
(50) Bicerano, J.; Clark, H. A. *Macromolecules* **1988**, *21*, 597.
(51) Sung, Y. J.; Chen, C. L.; Su, A. C. *Macromolecules* **1990**, *24*, 6123.
(52) Fried, J. R.; Letton, A.; Welch, W. J. *Polymer* **1990**, *31*, 1032.
(53) Perchak, D.; Skolnick, J.; Yaris, R. *Macromolecules* **1987**, *20*, 121.
(54) Chen, C. L.; Chen, H. L.; Lee, C. L.; Shih, J. H. *Macromolecules* **1994**, *27*, 2087.
(55) Fan, C. F.; Cagin, T.; Chen, Z. M.; Smith, K. A. *Macromolecules* **1994**, *27*, 2383.
(56) Clark, M.; Cramer, R. D., III; Van Opdenbosch, N. *J. Comput. Chem.* **1989**, *10*, 982.
(57) Beeman, D. J. *Comput. Phys.* **1976**, *20*, 130.

MA946267Y